Measurement of the ratio $\mathcal{B}(B^- \to D^{*0}K^-)/\mathcal{B}(B^- \to D^{*0}\pi^-)$ and of the *CP* asymmetry of $B^- \to D^{*0}_{CP+}K^-$ decays

B. Aubert,[1] R. Barate,[1] D. Boutigny,[1] F. Couderc,[1] Y. Karyotakis,[1] J. P. Lees,[1] V. Poireau,[1] V. Tisserand,[1] A. Zghiche,[1] E. Grauges-Pous,[2] A. Palano,[3] A. Pompili,[3] J. C. Chen,[4] N. D. Qi,[4] G. Rong,[4] P. Wang,[4] Y. S. Zhu,[4] G. Eigen,[5] I. Ofte,[5] B. Stugu,[5] G. S. Abrams,[6] A. W. Borgland,[6] A. B. Breon,[6] D. N. Brown,[6] J. Button-Shafer,[6] R. N. Cahn,[6] E. Charles,[6] C. T. Day,[6] M. S. Gill,[6] A. V. Gritsan,[6] Y. Groysman,[6] R. G. Jacobsen,[6] R. W. Kadel,[6] J. Kadyk,[6] L. T. Kerth,[6] Yu. G. Kolomensky,[6] G. Kukartsev,[6] G. Lynch,[6] L. M. Mir,[6] P. J. Oddone,[6] T. J. Orimoto,[6] M. Pripstein,[6] N. A. Roe,[6] M. T. Ronan,[6] W. A. Wenzel,[6] M. Barrett,[7] K. E. Ford,[7] T. J. Harrison,[7] A. J. Hart,[7] C. M. Hawkes,[7] S. E. Morgan,[7] A. T. Watson,[7] M. Fritsch,[8] K. Goetzen,[8] T. Held,[8] H. Koch,[8] B. Lewandowski,[8] M. Pelizaeus,[8] T. Schroeder,[8] M. Steinke,[8] J. T. Boyd,[9] N. Chevalier,[9] W. N. Cottingham,[9] M. P. Kelly,[9] T. E. Latham,[9] F. F. Wilson,[9] T. Cuhadar-Donszelmann,[10] C. Hearty,[10] N. S. Knecht,[10] T. S. Mattison,[10] J. A. McKenna,[10] D. Thiessen,[10] A. Khan,[11] P. Kyberd,[11] L. Teodorescu,[11] A. E. Blinov,[12] V. E. Blinov,[12] V. P. Druzhinin,[12] V. B. Golubev,[12] V. N. Ivanchenko,[12] E. A. Kravchenko,[12] A. P. Onuchin,[12] S. I. Serednyakov,[12] Yu. I. Skovpen,[12] E. P. Solodov,[12] A. N. Yushkov,[12] D. Best,[13] M. Bruinsma,[13] M. Chao,[13] I. Eschrich,[13] D. Kirkby,[13] A. J. Lankford,[13] M. Mandelkern,[13] R. K. Mommsen,[13] W. Roethel,[13] D. P. Stoker,[13] C. Buchanan,[14] B. L. Hartfiel,[14] A. J. R. Weinstein,[14] S. D. Foulkes,[15] J. W. Gary,[15] B. C. Shen,[15] K. Wang,[15] D. del Re,[16] H. K. Hadavand,[16] E. J. Hill,[16] D. B. MacFarlane,[16] H. P. Paar,[16] Sh. Rahatlou,[16] V. Sharma,[16] J. Adam Cunha,[17] J. W. Berryhill,[17] C. Campagnari,[17] B. Dahmes,[17] T. M. Hong,[17] A. Lu,[17] M. A. Mazur,[17] J. D. Richman,[17] W. Verkerke,[17] T. W. Beck,[18] A. M. Eisner,[18] C. A. Heusch,[18] J. Kroseberg,[18] W. S. Lockman,[18] G. Nesom,[18] T. Schalk,[18] B. A. Schumm,[18] A. Seiden,[18] P. Spradlin,[18] D. C. Williams,[18] M. G. Wilson,[18] J. Albert,[19] E. Chen,[19] G. P. Dubois-Felsmann,[19] A. Dvoretskii,[19] D. G. Hitlin,[19] I. Narsky,[19] T. Piatenko,[19] F. C. Porter,[19] A. Ryd,[19] A. Samuel,[19] S. Yang,[19] S. Jayatilleke,[20] G. Mancinelli,[20] B. T. Meadows,[20] M. D. Sokoloff,[20] F. Blanc,[21] P. Bloom,[21] S. Chen,[21] W. T. Ford,[21] U. Nauenberg,[21] A. Olivas,[21] P. Rankin,[21] W. O. Ruddick,[21] J. G. Smith,[21] K. A. Ulmer,[21] J. Zhang,[21] L. Zhang,[21] A. Chen,[22] E. A. Eckhart,[22] J. L. Harton,[22] A. Soffer,[22] W. H. Toki,[22] R. J. Wilson,[22] Q. Zeng,[22] B. Spaan,[23] D. Altenburg,[24] T. Brandt,[24] J. Brose,[24] M. Dickopp,[24] E. Feltresi,[24] A. Hauke,[24] H. M. Lacker,[24] R. Nogowski,[24] S. Otto,[24] A. Petzold,[24] J. Schubert,[24] K. R. Schubert,[24] R. Schwierz,[24] J. E. Sundermann,[24] D. Bernard,[25] G. R. Bonneaud,[25] P. Grenier,[25] S. Schrenk,[25] Ch. Thiebaux,[25] G. Vasileiadis,[25] M. Verderi,[25] D. J. Bard,[26] P. J. Clark,[26] F. Muheim,[26] S. Playfer,[26] Y. Xie,[26] M. Andreotti,[27] V. Azzolini,[27] D. Bettoni,[27] C. Bozzi,[27] R. Calabrese,[27] G. Cibinetto,[27] E. Luppi,[27] M. Negrini,[27] L. Piemontese,[27] A. Sarti,[27] F. Anulli,[28] R. Baldini-Ferroli,[28] A. Calcaterra,[28] R. de Sangro,[28] G. Finocchiaro,[28] P. Patteri,[28] I. M. Peruzzi,[28] M. Piccolo,[28] A. Zallo,[28] A. Buzzo,[29] R. Capra,[29] R. Contri,[29] G. Crosetti,[29] M. Lo Vetere,[29] M. Macri,[29] M. R. Monge,[29] S. Passaggio,[29] C. Patrignani,[29] E. Robutti,[29] A. Santroni,[29] S. Tosi,[29] S. Bailey,[30] G. Brandenburg,[30] K. S. Chaisanguanthum,[30] M. Morii,[30] E. Won,[30] R. S. Dubitzky,[31] U. Langenegger,[31] J. Marks,[31] U. Uwer,[31] W. Bhimji,[32] D. A. Bowerman,[32] P. D. Dauncey,[32] U. Egede,[32] J. R. Gaillard,[32] G. W. Morton,[32] J. A. Nash,[32] M. B. Nikolich,[32] G. P. Taylor,[32] M. J. Charles,[33] G. J. Grenier,[33] U. Mallik,[33] J. Cochran,[34] H. B. Crawley,[34] J. Lamsa,[34] W. T. Meyer,[34] S. Prell,[34] E. I. Rosenberg,[34] A. E. Rubin,[34] J. Yi,[34] N. Arnaud,[35] M. Davier,[35] X. Giroux,[35] G. Grosdidier,[35] A. Höcker,[35] F. Le Diberder,[35] V. Lepeltier,[35] A. M. Lutz,[35] T. C. Petersen,[35] S. Plaszczynski,[35] M. H. Schune,[35] G. Wormser,[35] C. H. Cheng,[36] D. J. Lange,[36] M. C. Simani,[36] D. M. Wright,[36] A. J. Bevan,[37] C. A. Chavez,[37] J. P. Coleman,[37] I. J. Forster,[37] J. R. Fry,[37] E. Gabathuler,[37] R. Gamet,[37] D. E. Hutchcroft,[37] R. J. Parry,[37] D. J. Payne,[37] C. Touramanis,[37] C. M. Cormack,[38] F. Di Lodovico,[38] C. L. Brown,[39] G. Cowan,[39] R. L. Flack,[39] H. U. Flaecher,[39] M. G. Green,[39] P. S. Jackson,[39] T. R. McMahon,[39] S. Ricciardi,[39] F. Salvatore,[39] M. A. Winter,[39] D. Brown,[40] C. L. Davis,[40] J. Allison,[41] N. R. Barlow,[41] R. J. Barlow,[41] M. C. Hodgkinson,[41] G. D. Lafferty,[41] J. C. Williams,[41] C. Chen,[42] A. Farbin,[42] W. D. Hulsbergen,[42] A. Jawahery,[42] D. Kovalskyi,[42] C. K. Lae,[42] V. Lillard,[42] D. A. Roberts,[42] G. Blaylock,[43] C. Dallapiccola,[43] S. S. Hertzbach,[43] R. Kofler,[43] V. B. Koptchev,[43] T. B. Moore,[43] S. Saremi,[43] H. Staengle,[43] S. Willocq,[43] R. Cowan,[44] K. Koeneke,[44] G. Sciolla,[44] S. J. Sekula,[44] F. Taylor,[44] R. K. Yamamoto,[44] D. J. J. Mangeol,[45] P. M. Patel,[45] S. H. Robertson,[45] A. Lazzaro,[46] V. Lombardo,[46] F. Palombo,[46] J. M. Bauer,[47] L. Cremaldi,[47] V. Eschenburg,[47] R. Godang,[47] R. Kroeger,[47] J. Reidy,[47] D. A. Sanders,[47] D. J. Summers,[47] H. W. Zhao,[47] S. Brunet,[48] D. Côté,[48] P. Taras,[48] H. Nicholson,[49] N. Cavallo,[50,*] F. Fabozzi,[50,*] C. Gatto,[50] L. Lista,[50] D. Monorchio,[50] P. Paolucci,[50] D. Piccolo,[50] C. Sciacca,[50] M. Baak,[51] H. Bulten,[51] G. Raven,[51] H. L. Snoek,[51] L. Wilden,[51] C. P. Jessop,[52] J. M. LoSecco,[52] T. Allmendinger,[53] K. K. Gan,[53] K. Honscheid,[53] D. Hufnagel,[53] H. Kagan,[53] R. Kass,[53] T. Pulliam,[53] A. M. Rahimi,[53] R. Ter-Antonyan,[53] Q. K. Wong,[53] J. Brau,[54] R. Frey,[54] O. Igonkina,[54] M. Lu,[54] C. T. Potter,[54] N. B. Sinev,[54] D. Strom,[54] E. Torrence,[54] F. Colecchia,[55] A. Dorigo,[55] F. Galeazzi,[55] M. Margoni,[55] M. Morandin,[55] M. Posocco,[55] M. Rotondo,[55]

F. Simonetto,[55] R. Stroili,[55] C. Voci,[55] M. Benayoun,[56] H. Briand,[56] J. Chauveau,[56] P. David,[56] Ch. de la Vaissière,[56] L. Del Buono,[56] O. Hamon,[56] M. J. J. John,[56] Ph. Leruste,[56] J. Malcles,[56] J. Ocariz,[56] L. Roos,[56] G. Therin,[56] P. K. Behera,[57] L. Gladney,[57] Q. H. Guo,[57] J. Panetta,[57] M. Biasini,[58] R. Covarelli,[58] M. Pioppi,[58] C. Angelini,[59] G. Batignani,[59] S. Bettarini,[59] M. Bondioli,[59] F. Bucci,[59] G. Calderini,[59] M. Carpinelli,[59] F. Forti,[59] M. A. Giorgi,[59] A. Lusiani,[59] G. Marchiori,[59] M. Morganti,[59] N. Neri,[59] E. Paoloni,[59] M. Rama,[59] G. Rizzo,[59] G. Simi,[59] J. Walsh,[59] M. Haire,[60] D. Judd,[60] K. Paick,[60] D. E. Wagoner,[60] N. Danielson,[61] P. Elmer,[61] Y. P. Lau,[61] C. Lu,[61] V. Miftakov,[61] J. Olsen,[61] A. J. S. Smith,[61] A. V. Telnov,[61] F. Bellini,[62] G. Cavoto,[61,62] R. Faccini,[62] F. Ferrarotto,[62] F. Ferroni,[62] M. Gaspero,[62] L. Li Gioi,[62] M. A. Mazzoni,[62] S. Morganti,[62] M. Pierini,[62] G. Piredda,[62] F. Safai Tehrani,[62] C. Voena,[62] S. Christ,[63] G. Wagner,[63] R. Waldi,[63] T. Adye,[64] N. De Groot,[64] B. Franek,[64] N. I. Geddes,[64] G. P. Gopal,[64] E. O. Olaiya,[64] R. Aleksan,[65] S. Emery,[65] A. Gaidot,[65] S. F. Ganzhur,[65] P.-F. Giraud,[65] G. Hamel de Monchenault,[65] W. Kozanecki,[65] M. Legendre,[65] G. W. London,[65] B. Mayer,[65] G. Schott,[65] G. Vasseur,[65] Ch. Yèche,[65] M. Zito,[65] M. V. Purohit,[66] A. W. Weidemann,[66] J. R. Wilson,[66] F. X. Yumiceva,[66] T. Abe,[67] D. Aston,[67] R. Bartoldus,[67] N. Berger,[67] A. M. Boyarski,[67] O. L. Buchmueller,[67] R. Claus,[67] M. R. Convery,[67] M. Cristinziani,[67] G. De Nardo,[67] J. C. Dingfelder,[67] D. Dong,[67] J. Dorfan,[67] D. Dujmic,[67] W. Dunwoodie,[67] S. Fan,[67] R. C. Field,[67] T. Glanzman,[67] S. J. Gowdy,[67] T. Hadig,[67] V. Halyo,[67] C. Hast,[67] T. Hryn'ova,[67] W. R. Innes,[67] M. H. Kelsey,[67] P. Kim,[67] M. L. Kocian,[67] D. W. G. S. Leith,[67] J. Libby,[67] S. Luitz,[67] V. Luth,[67] H. L. Lynch,[67] H. Marsiske,[67] R. Messner,[67] D. R. Muller,[67] C. P. O'Grady,[67] V. E. Ozcan,[67] A. Perazzo,[67] M. Perl,[67] B. N. Ratcliff,[67] A. Roodman,[67] A. A. Salnikov,[67] R. H. Schindler,[67] J. Schwiening,[67] A. Snyder,[67] A. Soha,[67] J. Stelzer,[67] J. Strube,[54,67] D. Su,[67] M. K. Sullivan,[67] J. Va'vra,[67] S. R. Wagner,[67] M. Weaver,[67] W. J. Wisniewski,[67] M. Wittgen,[67] D. H. Wright,[67] A. K. Yarritu,[67] C. C. Young,[67] P. R. Burchat,[68] A. J. Edwards,[68] S. A. Majewski,[68] B. A. Petersen,[68] C. Roat,[68] M. Ahmed,[69] S. Ahmed,[69] M. S. Alam,[69] J. A. Ernst,[69] M. A. Saeed,[69] M. Saleem,[69] F. R. Wappler,[69] W. Bugg,[70] M. Krishnamurthy,[70] S. M. Spanier,[70] R. Eckmann,[71] H. Kim,[71] J. L. Ritchie,[71] A. Satpathy,[71] R. F. Schwitters,[71] J. M. Izen,[72] I. Kitayama,[72] X. C. Lou,[72] S. Ye,[72] F. Bianchi,[73] M. Bona,[73] F. Gallo,[73] D. Gamba,[73] L. Bosisio,[74] C. Cartaro,[74] F. Cossutti,[74] G. Della Ricca,[74] S. Dittongo,[74] S. Grancagnolo,[74] L. Lanceri,[74] P. Poropat,[74,†] L. Vitale,[74] G. Vuagnin,[74] F. Martinez-Vidal,[2,75] R. S. Panvini,[76] Sw. Banerjee,[77] B. Bhuyan,[77] C. M. Brown,[77] D. Fortin,[77] P. D. Jackson,[77] R. Kowalewski,[77] J. M. Roney,[77] R. J. Sobie,[77] J. J. Back,[78] P. F. Harrison,[78] G. B. Mohanty,[78] H. R. Band,[79] X. Chen,[79] B. Cheng,[79] S. Dasu,[79] M. Datta,[79] A. M. Eichenbaum,[79] K. T. Flood,[79] M. Graham,[79] J. J. Hollar,[79] J. R. Johnson,[79] P. E. Kutter,[79] H. Li,[79] R. Liu,[79] A. Mihalyi,[79] Y. Pan,[79] R. Prepost,[79] P. Tan,[79] J. H. von Wimmersperg-Toeller,[79] J. Wu,[79] S. L. Wu,[79] Z. Yu,[79] M. G. Greene,[80] and H. Neal[80]

(*BABAR* Collaboration)

[1]*Laboratoire de Physique des Particules, F-74941 Annecy-le-Vieux, France*
[2]*Universidad Autonoma de Barcelona, E-08193 Bellaterra, Barcelona, Spain*
[3]*Università di Bari, Dipartimento di Fisica and INFN, I-70126 Bari, Italy*
[4]*Institute of High Energy Physics, Beijing 100039, China*
[5]*University of Bergen, Inst. of Physics, N-5007 Bergen, Norway*
[6]*Lawrence Berkeley National Laboratory and University of California, Berkeley, California 94720, USA*
[7]*University of Birmingham, Birmingham, B15 2TT, United Kingdom*
[8]*Ruhr Universität Bochum, Institut für Experimentalphysik 1, D-44780 Bochum, Germany*
[9]*University of Bristol, Bristol BS8 1TL, United Kingdom*
[10]*University of British Columbia, Vancouver, BC, Canada V6T 1Z1*
[11]*Brunel University, Uxbridge, Middlesex UB8 3PH, United Kingdom*
[12]*Budker Institute of Nuclear Physics, Novosibirsk 630090, Russia*
[13]*University of California at Irvine, Irvine, California 92697, USA*
[14]*University of California at Los Angeles, Los Angeles, California 90024, USA*
[15]*University of California at Riverside, Riverside, California 92521, USA*
[16]*University of California at San Diego, La Jolla, California 92093, USA*
[17]*University of California at Santa Barbara, Santa Barbara, California 93106, USA*
[18]*University of California at Santa Cruz, Institute for Particle Physics, Santa Cruz, California 95064, USA*
[19]*California Institute of Technology, Pasadena, California 91125, USA*
[20]*University of Cincinnati, Cincinnati, Ohio 45221, USA*
[21]*University of Colorado, Boulder, Colorado 80309, USA*
[22]*Colorado State University, Fort Collins, Colorado 80523, USA*
[23]*Universität Dortmund, Institut fur Physik, D-44221 Dortmund, Germany*
[24]*Technische Universität Dresden, Institut für Kern- und Teilchenphysik, D-01062 Dresden, Germany*

^{25}Ecole Polytechnique, LLR, F-91128 Palaiseau, France

^{26}University of Edinburgh, Edinburgh EH9 3JZ, United Kingdom

^{27}Università di Ferrara, Dipartimento di Fisica and INFN, I-44100 Ferrara, Italy

^{28}Laboratori Nazionali di Frascati dell'INFN, I-00044 Frascati, Italy

^{29}Università di Genova, Dipartimento di Fisica and INFN, I-16146 Genova, Italy

^{30}Harvard University, Cambridge, Massachusetts 02138, USA

^{31}Universität Heidelberg, Physikalisches Institut, Philosophenweg 12, D-69120 Heidelberg, Germany

^{32}Imperial College London, London, SW7 2AZ, United Kingdom

^{33}University of Iowa, Iowa City, Iowa 52242, USA

^{34}Iowa State University, Ames, Iowa 50011-3160, USA

^{35}Laboratoire de l'Accélérateur Linéaire, F-91898 Orsay, France

^{36}Lawrence Livermore National Laboratory, Livermore, California 94550, USA

^{37}University of Liverpool, Liverpool L69 72E, United Kingdom

^{38}Queen Mary, University of London, E1 4NS, United Kingdom

^{39}University of London, Royal Holloway and Bedford New College, Egham, Surrey TW20 0EX, United Kingdom

^{40}University of Louisville, Louisville, Kentucky 40292, USA

^{41}University of Manchester, Manchester M13 9PL, United Kingdom

^{42}University of Maryland, College Park, Maryland 20742, USA

^{43}University of Massachusetts, Amherst, Massachusetts 01003, USA

^{44}Massachusetts Institute of Technology, Laboratory for Nuclear Science, Cambridge, Massachusetts 02139, USA

^{45}McGill University, Montréal, QC, Canada H3A 2T8

^{46}Università di Milano, Dipartimento di Fisica and INFN, I-20133 Milano, Italy

^{47}University of Mississippi, University, Mississippi 38677, USA

^{48}Université de Montréal, Laboratoire René J. A. Lévesque, Montréal, QC, Canada H3C 3J7

^{49}Mount Holyoke College, South Hadley, Massachusetts 01075, USA

^{50}Università di Napoli Federico II, Dipartimento di Scienze Fisiche and INFN, I-80126, Napoli, Italy

^{51}NIKHEF, National Institute for Nuclear Physics and High Energy Physics, NL-1009 DB Amsterdam, The Netherlands

^{52}University of Notre Dame, Notre Dame, Indiana 46556, USA

^{53}Ohio State University, Columbus, Ohio 43210, USA

^{54}University of Oregon, Eugene, Oregon 97403, USA

^{55}Università di Padova, Dipartimento di Fisica and INFN, I-35131 Padova, Italy

^{56}Universités Paris VI et VII, Laboratoire de Physique Nucléaire et de Hautes Energies, F-75252 Paris, France

^{57}University of Pennsylvania, Philadelphia, Pennsylvania 19104, USA

^{58}Università di Perugia, Dipartimento di Fisica and INFN, I-06100 Perugia, Italy

^{59}Università di Pisa, Dipartimento di Fisica, Scuola Normale Superiore and INFN, I-56127 Pisa, Italy

^{60}Prairie View A&M University, Prairie View, Texas 77446, USA

^{61}Princeton University, Princeton, New Jersey 08544, USA

^{62}Università di Roma La Sapienza, Dipartimento di Fisica and INFN, I-00185 Roma, Italy

^{63}Universität Rostock, D-18051 Rostock, Germany

^{64}Rutherford Appleton Laboratory, Chilton, Didcot, Oxon, OX11 0QX, United Kingdom

^{65}DSM/Dapnia, CEA/Saclay, F-91191 Gif-sur-Yvette, France

^{66}University of South Carolina, Columbia, South Carolina 29208, USA

^{67}Stanford Linear Accelerator Center, Stanford, California 94309, USA

^{68}Stanford University, Stanford, California 94305-4060, USA

^{69}State University of New York, Albany, New York 12222, USA

^{70}University of Tennessee, Knoxville, Tennessee 37996, USA

^{71}University of Texas at Austin, Austin, Texas 78712, USA

^{72}University of Texas at Dallas, Richardson, Texas 75083, USA

^{73}Università di Torino, Dipartimento di Fisica Sperimentale and INFN, I-10125 Torino, Italy

^{74}Università di Trieste, Dipartimento di Fisica and INFN, I-34127 Trieste, Italy

^{75}Universidad de Valencia, E-46100 Burjassot, Valencia, Spain

^{76}Vanderbilt University, Nashville, Tennessee 37235, USA

^{77}University of Victoria, Victoria, BC, Canada V8W 3P6

^{78}Department of Physics, University of Warwick, Coventry CV4 7AL, United Kingdom

^{79}University of Wisconsin, Madison, Wisconsin 53706, USA

^{80}Yale University, New Haven, Connecticut 06511, USA

---

*Also with Università della Basilicata, Potenza, Italy

†Deceased

RAPID COMMUNICATIONS

B. AUBERT et al.   PHYSICAL REVIEW D **71,** 031102 (2005)

We study the decays $B^- \to D^{*0}\pi^-$ and $B^- \to D^{*0}K^-$, where the D^{*0} decays into $D^0\pi^0$, with the D^0 reconstructed in the CP-even ($CP+$) eigenstates K^-K^+ and $\pi^-\pi^+$ and in the (non-CP) channels $K^-\pi^+$, $K^-\pi^+\pi^+\pi^-$, and $K^-\pi^+\pi^0$. Using a sample of about 123×10^6 $B\bar{B}$ pairs, we measure the ratios of decay rates $R^*_{\text{non}-CP} \equiv \frac{\mathcal{B}(B^- \to D^{*0}_{\text{non}-CP}K^-)}{\mathcal{B}(B^- \to D^{*0}_{\text{non}-CP}\pi^-)} = 0.0813 \pm 0.0040(\text{stat})^{+0.0042}_{-0.0031}(\text{syst})$, and provide the first measurements

of $R^*_{CP+} \equiv \frac{\mathcal{B}(B^- \to D^{*0}_{CP+}K^-)}{\mathcal{B}(B^- \to D^{*0}_{CP+}\pi^-)} = 0.086 \pm 0.021(\text{stat}) \pm 0.007(\text{syst})$, and of the CP asymmetry

$A^*_{CP+} \equiv \frac{\mathcal{B}(B^- \to D^{*0}_{CP+}K^-) - \mathcal{B}(B^+ \to D^{*0}_{CP+}K^+)}{\mathcal{B}(B^- \to D^{*0}_{CP+}K^-) + \mathcal{B}(B^+ \to D^{*0}_{CP+}K^+)} = -0.10 \pm 0.23(\text{stat})^{+0.03}_{-0.04}(\text{syst})$.

The decays $B^- \to D^{(*)0}K^{(*)-}$ will play an important role in our understanding of CP violation, as they can be used to constrain the angle $\gamma = \arg(-V_{ud}V^*_{ub}/V_{cd}V^*_{cb})$ of the Cabibbo-Kobayashi-Maskawa (CKM) matrix in a theoretically clean way by exploiting the interference between the $b \to c\bar{u}s$ and $b \to u\bar{c}s$ decay amplitudes [1]. In the standard model, neglecting $D^0\bar{D}^0$ mixing, $R^*_{CP\pm}/R^*_{\text{non}-CP} \simeq 1 + r^2 \pm 2r\cos\delta\cos\gamma$, where $CP+(-)$ indicates CP-even (odd) modes,

$$R^*_{\text{non}-CP/CP\pm} \equiv \frac{\mathcal{B}(B^- \to D^{*0}_{\text{non}-CP/CP\pm}K^-)}{\mathcal{B}(B^- \to D^{*0}_{\text{non}-CP/CP\pm}\pi^-)}, \quad (1)$$

r is the absolute value of the ratio of the color suppressed $B^+ \to D^{*0}K^+$ and color allowed $B^- \to D^{*0}K^-$ amplitudes ($r \sim 0.1$–0.3), and δ is the strong phase difference between those amplitudes. The decays $B^- \to D^{*0}\pi^-$ provide a convenient normalization term since many systematic uncertainties are common to the two, while the interference effects should be highly suppressed for the $D^{*0}\pi^-$ when compared to the ones for the $D^{*0}K^-$ final states. Furthermore, defining the direct CP asymmetry

$$A^*_{CP\pm} \equiv \frac{\mathcal{B}(B^- \to D^{*0}_{CP\pm}K^-) - \mathcal{B}(B^+ \to D^{*0}_{CP\pm}K^+)}{\mathcal{B}(B^- \to D^{*0}_{CP\pm}K^-) + \mathcal{B}(B^+ \to D^{*0}_{CP\pm}K^+)}, \quad (2)$$

we have: $A^*_{CP\pm} = \pm 2r\sin\delta\sin\gamma/(1 + r^2 \pm 2r\cos\delta\cos\gamma)$. The unknowns δ, r, and γ can be constrained by measuring $R^*_{\text{non}-CP}$, $R^*_{CP\pm}$, and $A^*_{CP\pm}$. The Belle Collaboration has reported $R^*_{\text{non}-CP} = 0.078 \pm 0.019 \pm 0.009$ using 10.1 fb^{-1} of data [2].

We present the measurement of $R^*_{\text{non}-CP}$, R^*_{CP+} and A^*_{CP+} performed using 113 fb^{-1} of data taken at the $\Upsilon(4S)$ resonance by the *BABAR* detector with the PEP-II asymmetric B factory. An additional 12 fb^{-1} of data taken at a center-of-mass (CM) energy 40 MeV below the $\Upsilon(4S)$ mass was used for background studies. The *BABAR* detector is described in detail elsewhere [3]. Tracking of charged particles is provided by a five-layer silicon vertex tracker (SVT) and a 40-layer drift chamber (DCH). The particle identification exploits ionization energy loss in the DCH and SVT, and Cherenkov photons detected in a ring-imaging detector (DIRC). An electromagnetic calorimeter (EMC), comprised of 6580 thallium-doped CsI crystals, is used to identify electrons and photons. These systems are mounted inside a 1.5-T solenoidal superconducting mag-

net. Finally, the instrumented flux return (IFR) of the magnet allows discrimination of muons from other particles. We use the GEANT4 Monte Carlo (MC) [4] program to simulate the response of the detector, taking into account the varying accelerator and detector conditions.

We reconstruct $B^- \to D^{*0}h^-$ candidates, where the prompt track h^- is a kaon or a pion. D^{*0} candidates are reconstructed from $D^{*0} \to D^0\pi^0$ decays and D^0 mesons from their decays to $K^-\pi^+$, $K^-\pi^+\pi^+\pi^-$, $K^-\pi^+\pi^0$, $\pi^-\pi^+$, and K^-K^+. The first three modes are referred to as "non-CP modes", the last two as "CP modes". Reference to the charge-conjugate decays is implied here and throughout the text, unless otherwise stated.

Charged tracks used in the reconstruction of D and B meson candidates must have a distance of closest approach to the interaction point less than 1.5 cm in the transverse plane and less than 10 cm along the beam axis. Charged tracks from the $D^0 \to \pi^-\pi^+$ decay must also have transverse momenta greater than 0.1 GeV/c and total momenta in the CM frame greater than 0.25 GeV/c. Kaon and pion candidates from all D^0 decays must pass particle identification (PID) selection criteria, based on a neural-network algorithm which uses measurements of dE/dx in the DCH and the SVT, and Cherenkov photons in the DIRC.

For the prompt track to be identified as a pion or a kaon, we require that its Cherenkov angle (θ_C) be reconstructed with at least five photons. To suppress misreconstructed tracks while maintaining high efficiency, events with prompt tracks with θ_C more than 2 standard deviations (s.d.) away from the expected values for both the kaon and pion hypotheses are discarded; this selection rejects most protons as well. The track is also discarded if it is identified with high probability as an electron or a muon.

Neutral pions are reconstructed by combining pairs of photons with energy deposits larger than 30 MeV in the calorimeter that are not matched to charged tracks. The $\gamma\gamma$ invariant mass is required to be in the range 122–146 MeV/c^2. The mass resolution for neutral pions is typically 6–7 MeV/c^2. The minimum total laboratory energy required for the $\gamma\gamma$ combinations is set to 200 MeV for π^0 candidates from D^0 mesons. Only π^0 candidates with CM momenta in the range 70–450 MeV/c (denoted as soft pions, π_s) are used to reconstruct the D^{*0}.

The D^0 mass resolution is 11 MeV/c^2 for the $D^0 \to K^-\pi^+\pi^0$ mode and about 7 MeV/c^2 for all other modes.

A mass-constrained fit is applied to the D candidate. The resolution of the difference between the masses of the D^{*0} and the daughter D^0 candidates (ΔM) is typically in the range 0.8–1.0 MeV/c^2, depending on the D^0 decay mode. A combined cut on the measured D^0 and soft-pion invariant masses and on ΔM is also applied by means of a χ^2 defined as:

$$\chi^2 \equiv \left| \frac{m_{D^0} - \overline{m}_{D^0}}{\sigma_{m_{D^0}}} \right|^2 + \left| \frac{m_{\pi_s} - \overline{m}_{\pi_s}}{\sigma_{m_{\pi_s}}} \right|^2 + \left| \frac{\Delta M - \overline{\Delta M}}{\sigma_{\Delta M}} \right|^2,$$

(3)

where the mean values ($\overline{m}_{D^0}$, $\overline{m}_{\pi_s}$, $\overline{\Delta M}$) and the resolutions ($\sigma_{m_{D^0}}$, $\sigma_{m_{\pi_s}}$, $\sigma_{\Delta M}$) are measured in the data. Correlations between the observables used in the χ^2 in Eq. (3) are negligible. Events with $\chi^2 > 9$ are rejected.

B meson candidates are reconstructed by combining a D^{*0} candidate with a high-momentum charged track. For the non-CP modes, the charge of the prompt track h must match that of the kaon from the D^0 meson decay. Two quantities are used to discriminate between signal and background: the beam-energy-substituted mass $m_{ES} \equiv \sqrt{(E_i^{*2}/2 + \mathbf{p}_i \cdot \mathbf{p}_B)^2/E_i^2 - p_B^2}$ and the energy difference $\Delta E \equiv E_B^* - E_i^*/2$, where the subscripts i and B refer to the initial e^+e^- system and the B candidate, respectively, and the asterisk denotes the CM frame.

The m_{ES} distribution for the $B^- \to D^{*0}h^-$ signal can be described by a Gaussian function centered at the B mass and does not depend on the nature of the prompt track. Its resolution, about 2.6 MeV/c^2, is dominated by the uncertainty of the beam energy and is slightly dependent on the D^0 decay mode. The observable ΔE does depend on the mass assigned to the tracks forming the B candidate, and on the D^0 momentum resolution. We calculate ΔE with the kaon hypothesis for the prompt track and indicate this quantity with ΔE_K. For $B^- \to D^{*0}K^-$ events ΔE_K is described approximately by a Gaussian centered at zero and with resolution 17–18 MeV, whereas for $B^- \to D^{*0}\pi^-$ events ΔE_K is shifted positively by about 50 MeV. B candidates with m_{ES} in the range 5.2–5.3 GeV/c^2 and with ΔE_K in the range (-100 to 130) MeV are selected.

A large fraction of the background consists of continuum (non $B\overline{B}$) events and a powerful set of selection criteria is needed to suppress it. The selection is chosen to maximize the expected significance of the results, based on MC studies. In the CM frame, this background typically has two-jet structure, while $B\overline{B}$ events are isotropic. We define θ_T as the angle between the thrust axes of the B candidate and of the remaining charged and neutral particles in the event, both evaluated in the CM frame, and signed so that the thrust axis component along the e^- beam direction is positive. The distribution of $|\cos\theta_T|$ is strongly peaked near one for continuum events and is approximately uniform for $B\overline{B}$ events. For the non-CP modes, $|\cos\theta_T|$ is required to be less than 0.9 for the $D^0 \to$ $K^-\pi^+$ mode, and less than 0.85 for $D^0 \to K^-\pi^+\pi^+\pi^-$ and $D^0 \to K^-\pi^+\pi^0$ modes for which the levels of the continuum background are higher. For the CP modes, $\cos\theta_T$ is required to be in the ranges (-0.9 to 0.85) and (-0.85 to 0.8) for the $D^0 \to K^-K^+$ and $D^0 \to \pi^-\pi^+$ modes, respectively. Other mode-dependent selection criteria are applied: for the $D^0 \to K^-\pi^+\pi^+\pi^-$ and $D^0 \to K^-\pi^+\pi^0$ ($D^0 \to \pi^-\pi^+$) modes we reject events with $\cos\theta_{tD} < -0.9$ ($|\cos\theta_{tD}| > 0.95$), where θ_{tD} is the angle between the direction of the D^0 in the laboratory and the opposite of the direction of the K^- (π^- for the $D^0 \to \pi^-\pi^+$ mode) from the D^0 in the D^0 rest frame. Finally, to reduce combinatorial background in the $D^0 \to K^-\pi^+\pi^0$ final state, only those events that fall in the enhanced regions of the Dalitz plots, according to the results of the Fermilab E691 experiment [5], are selected. This last requirement alone rejects 80% of the background and accepts 69% of the signal, according to the MC simulation.

Multiple candidates are found in about 10%–12% of the selected events with two- and four-body D^0 decays and in 17% of the events with $D^0 \to K^-\pi^+\pi^0$ decays. The best candidate in each event is selected based on the χ^2 previously defined. The number of candidates constructed with the same D^{*0}, but different prompt track, is negligible; in this rare case the best one in the event is randomly chosen. The reconstruction efficiencies, based on MC simulation, are reported in Table I.

According to the simulation, the main contributions to the $B\overline{B}$ background for $B^- \to D^{*0}h^-$ events originate from the decays $B^- \to D^{(*)0}\rho^-$ and $B^0 \to D^{*-}h^+$. $B^- \to D^{*0}(\to D^0\gamma)h^-$ events are also considered background as their CP modes have CP eigenvalues opposite to the ones of the $B^- \to D^{*0}h^-$ signal [6].

For each D^0 decay mode, an unbinned maximum-likelihood (ML) fit is used to extract yields from the data for six candidate types: signal, continuum background, and $B\overline{B}$ background, for the kaon and pion choices for the mass hypothesis of the prompt track in the candidate decays $B^- \to D^{*0}h^-$.

TABLE I. Results of the yields from the ML fit. For the CP modes the results of the fit separately for the B^+ and B^- samples are also quoted. Errors are statistical only. The efficiencies (ϵ) based on MC simulation are also reported.

D^0 mode	$N(B \to D^{*0}\pi)$	$N(B \to D^{*0}K)$	$\epsilon(D^{*0}\pi)$ (%)
$K^-\pi^+$	2639 ± 56	226 ± 18	17.5 ± 0.2
$K^-\pi^+\pi^0$	3249 ± 68	247 ± 21	5.9 ± 0.1
$K^-\pi^+\pi^+\pi^-$	3071 ± 64	242 ± 21	9.7 ± 0.1
K^-K^+	258 ± 19	23.4 ± 5.6	15.3 ± 0.2
$K^-K^+ [B^+]$	123 ± 13	13.4 ± 4.1	15.6 ± 0.3
$K^-K^+ [B^-]$	134 ± 13	9.9 ± 3.7	14.9 ± 0.3
$\pi^-\pi^+$	124 ± 14	6.3 ± 4.6	14.6 ± 0.2
$\pi^-\pi^+ [B^+]$	75 ± 11	0.7 ± 3.2	14.5 ± 0.3
$\pi^-\pi^+ [B^-]$	49 ± 9	5.3 ± 3.5	14.8 ± 0.3

Three quantities from each selected candidate are used as input to the fit: ΔE_K, m_{ES}, and the θ_C of the prompt track. The distributions of ΔE_K and m_{ES} for the six candidate types are parametrized to build the probability density functions (PDFs) that are used in the fit.

Correlations between the m_{ES} and ΔE_K variables for signal events are about -5% according to the simulation. To account for these, we use signal MC events to parametrize the signal PDFs with a method based on kernel estimation [7], which allows the description of a two-dimensional PDF. The shapes of MC and data distributions of these observables are in good agreement, according to comparisons performed with pure samples of $B^- \to D^{*0}\pi^-$ events, obtained with very tight particle identification and kinematic selection. To the extent that we find differences in the data and MC distributions, we adjust the shapes of the PDFs to conform to the data. Systematic uncertainties due to limited statistics associated with this procedure are included in the final results.

We obtain the PDFs for the m_{ES} distribution for continuum background from off-resonance data, applying the standard selection criteria. The m_{ES} distributions are parametrized with a threshold function [8] defined as $f(m_{ES}) \propto y\sqrt{1-y^2}\exp[-\xi(1-y^2)]$, where $y = m_{ES}/m_0$ and m_0 is the mean energy of the beams in the CM frame. The PDFs for the ΔE_K distributions for background candidates from the continuum are well-parametrized with exponential functions whose parameters are determined by fitting the ΔE_K distributions of the selected $B^- \to D^{*0}h^-$ sample in the off-resonance data. Both the m_{ES} and the ΔE_K PDFs for the continuum background are taken to be the same for $B^- \to D^{*0}\pi^-$ and $B^- \to D^{*0}K^-$ decays. The shapes of MC and data distributions of m_{ES} and ΔE_K obtained with looser selection criteria to increase the statistics, agree well for $B^- \to D^{*0}\pi^-$ and $B^- \to D^{*0}K^-$ decays, validating this assumption. For the CP modes very few off-resonance events pass the selection criteria, hence we use the PDFs determined for the $D^0 \to K^-\pi^+$ mode. This is justified by a separate comparison of the CP modes with the flavor-definite modes in data and MC samples obtained with looser selection criteria.

The correlation between m_{ES} and ΔE_K for the $B\overline{B}$ background is taken into account with a two-dimensional PDF determined from simulated events, in a similar way to that used for the signal.

We obtain PDFs for the particle identification determination for the prompt track from the distributions, in bins of momentum and polar angle, of the difference between the reconstructed and expected θ_C of kaons and pions from D^0 decays in a control sample that exploits the decay chain $D^{*+} \to D^0\pi^+$, $D^0 \to K^-\pi^+$ to identify the tracks kinematically.

Initial PDFs are parametrized for each candidate type as detailed above. With these we then fit pure samples of simulated signal events and of background from off-

resonance real and MC data. With the yields from these fits we establish an efficiency matrix accounting for small cross feeds among the components. The corrections affecting the signal yields are typically of order 1%. The fractional systematic uncertainties for the signal yields associated with these corrections are in the range 0.1%–6.0% depending on the D^0 decay mode.

The likelihood $\mathcal{L}$ for the selected sample is given by the product of the final PDFs for each individual candidate and a Poisson factor:

$$\mathcal{L} \equiv \frac{e^{-N'}(N')^N}{N!} \prod_{i=1}^{N} \sum_{j=1}^{6} \frac{N_j}{N'} \mathcal{P}_j(m_{ES_i}, \Delta E_{K_i}, \theta_{C_i}) \qquad (4)$$

where N is the total number of events, N_j are the yields for each of the previously defined six candidate types, and $N' \equiv \sum_{j=1}^{6} N_j$, $\mathcal{P}_j(m_{ES_i}, \Delta E_{K_i}, \theta_{C_i})$ is the probability to measure the particular set of physical quantities $(m_{ES_i}, \Delta E_{K_i}, \theta_{C_i})$ in the ith event for a candidate of type j. The Poisson factor is the probability of observing N total events when N' are expected. The quantity $\mathcal{L}$ is maximized with respect to the six yields using the MINUIT program [9]. The fit has also been performed on luminosity-weighted MC and high statistics toy MC events and it has been found to be unbiased.

The results of the fit are reported in detail in Table I. These yields are used to determine the CP asymmetry parameters. We measure:

$$R^*_{\text{non}-CP} = 0.0813 \pm 0.0040(\text{stat})^{+0.0042}_{-0.0031}(\text{syst}),$$

$$R^*_{CP+} = 0.086 \pm 0.021(\text{stat}) \pm 0.007(\text{syst}),$$

$$R^*_{CP+}/R^*_{\text{non}-CP} = 1.06 \pm 0.26(\text{stat})^{+0.10}_{-0.09}(\text{syst}),$$

$$A^*_{CP+} = -0.10 \pm 0.23(\text{stat})^{+0.03}_{-0.04}(\text{syst}).$$

Figure 1 shows the distributions of ΔE_K for the combined non-CP and CP modes before and after the enhancement of the $B \to D^{*0}K$ component. The enhancement is accomplished by requiring that the prompt track be consistent with the kaon hypothesis and that $m_{ES} > 5.27$ GeV/c^2. The ΔE_K projections of the fit results are also shown.

The ratio of the decay rates for $B^- \to D^{*0}\pi^-$ and $B^- \to D^{*0}K^-$ is separately calculated for the different D^0 decay channels and is computed with the signal yields estimated with the ML fit and listed in Table I. The resulting ratios are scaled by correction factors of a few percent, which are estimated with simulated data and which take into account small differences in the efficiency between $B^- \to D^{*0}K^-$ and $B^- \to D^{*0}\pi^-$ event selections. The results are listed in Table II.

The sources of systematic uncertainties for the yields have been identified and their contributions (for the measurement of $R^*_{(\text{non}-)CP}$) are reported in Table III. Uncertainties of the signal parametrizations of ΔE_K and m_{ES} arise from the assumed shapes of the PDFs and dis-
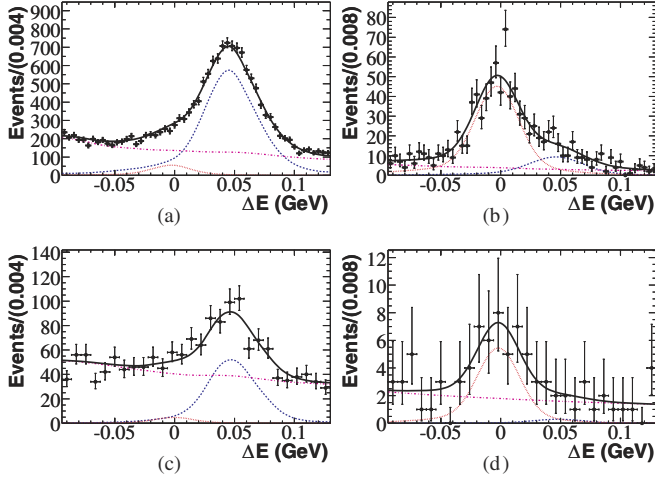
RAPID COMMUNICATIONS

MEASUREMENT OF THE RATIO $\mathcal{B}(B^- \to D^{*0}K^-)/\mathcal{B}(B^- \to D^{*0}\pi^-)$ ... PHYSICAL REVIEW D **71,** 031102 (2005)

FIG. 1 (color online). Distributions of ΔE_K in the $B \to D^{*0}h$ sample, for $D^0 \to K^- \pi^+, K^- \pi^+ \pi^0, K^- \pi^+ \pi^+ \pi^-$ [(a),(b)] and $D^0 \to K^- K^+, \pi^- \pi^+$ [(c),(d)], before [(a),(c)] and after [(b),(d)] enhancing the $B \to D^{*0}K$ component by requiring that the prompt track be consistent with the kaon hypothesis and $m_{ES} >$ 5.27 GeV/c^2. The $B^- \to D^{*0}\pi^-$ signal contribution on the right of each plot is shown as a dashed line, the $B^- \to D^{*0}K^-$ signal on the left as a dotted line, and the background as a dashed-dotted line. The total fit with all the contributions is shown with a thick solid line.

crepancies between real and simulated data. All of the parameters of the ΔE_K and m_{ES} PDFs have also been varied according to their 1 s.d. statistical uncertainties and signed variations in the yields are taken as systematic uncertainties. For the $B\bar{B}$ and continuum backgrounds, the systematic uncertainties due to the limited statistics of the MC and of the off-resonance data have been calculated varying the ΔE_K and m_{ES} PDF parameters by their statistical uncertainties. There are several contributions to the PID systematic uncertainty for the prompt track: the uncertainty due to limited statistics is calculated by varying each parameter of the PDF, in each bin in momentum and polar angle, by its uncertainty (keeping constant all other parameters in the same bin and all parameters in all the other bins) and summing all the contributions in quadra-

ture; results obtained with alternative PID PDFs, which account for different θ_C residual shapes and for discrepancies between data and simulation, are also included as systematic uncertainties. The systematic uncertainties due to the fit cross feeds have been evaluated. Finally, errors associated with the efficiency correction factor are also included.

Many of the systematic uncertainties for the signal yields have similar effects on the $B^- \to D^{*0}K^-$ and $B^- \to D^{*0}\pi^-$ events (they increase or decrease both fractions simultaneously), hence their effect is reduced in deriving the systematic uncertainty for the measurement of the ratios, when all correlations are taken into account. Overall, the main sources of systematic uncertainties for the measurement of both $R^*_{(\text{non}-)CP}$ and A^*_{CP+} are due to the characterization of the shapes of m_{ES} and ΔE_K for the signal, to the characterization of the m_{ES} PDFs for the background, to the particle identification, and to the uncertainty of the fit cross feeds and of the efficiency correction factors. The systematic uncertainty for A^*_{CP+} due to possible detector charge asymmetries is evaluated by measuring asymmetries analogous to those defined in Eq. (2), but for $B^- \to D^{*0}\pi^-$ and $B^- \to D^{*0}K^-$ events (the latter uniquely for the non-CP modes), where CP violation is expected to be negligible. Results for all modes are then combined, taking correlations into account. The measured asymmetry is -0.008 ± 0.012(stat) ± 0.001(syst). Though it is consistent with zero, it is also consistent with -0.020 at 1 s.d. level, hence we take the magnitude of this value as a further symmetric systematic uncertainty on A^*_{CP+}. When combining the results for the different modes, all systematic and statistical uncertainties are considered to be uncorrelated, except for the contributions of the PID PDF (common to all modes) and of the detector charge asymmetry in the measurement of A^*_{CP+}, which are considered to be completely correlated. For the measurement of $R^*_{CP+}/R^*_{\text{non}-CP}$ all systematic uncertainties have been considered to be uncorrelated; this assumption is

TABLE II. Measured ratios for different D^0 decay modes. The first error is statistical, the second is systematic.

$B^- \to D^{*0}h^-$ Mode	$\mathcal{B}(B \to D^{*0}K)/\mathcal{B}(B \to D^{*0}\pi)$ (%)
$D^0 \to K^- \pi^+$	$8.93 \pm 0.72^{+0.38}_{-0.30}$
$D^0 \to K^- \pi^+ \pi^0$	$7.59 \pm 0.65^{+0.37}_{-0.27}$
$D^0 \to K^- \pi^+ \pi^+ \pi^-$	$7.91 \pm 0.72^{+0.61}_{-0.59}$
Weighted mean (non-CP)	$8.13 \pm 0.40^{+0.42}_{-0.31}$
$D^0 \to K^- K^+$	$9.4 \pm 2.3 \pm 0.6$
$D^0 \to \pi^- \pi^+$	$5.9 \pm 4.4^{+1.0}_{-1.4}$
Weighted mean (CP)	$8.6 \pm 2.1 \pm 0.7$

TABLE III. Average systematic uncertainties for $R^*_{(\text{non}-)CP}$.

Systematic source	$\Delta R^*_{\text{non}-CP}/R^*_{\text{non}-CP}$ (%) non-CP modes	$\Delta R^*_{CP}/R^*_{CP}$ (%) CP modes
ΔE_K (signal)	$+2.0$ -1.8	$+2.7$ -2.8
$\Delta E_K(q\bar{q})$	$+0.3$ -0.6	$+0.9$ -2.5
$\Delta E_K(B\bar{B})$	$+0.0$ -0.5	$+0.8$ -0.8
m_{ES}(signal)	$+0.4$ -0.3	$+0.7$ -0.4
$m_{ES}(q\bar{q})$	$+0.8$ -0.8	$+4.4$ -6.7
$m_{ES}(B\bar{B})$	$+1.2$ -1.3	$+0.3$ -3.2
PDF cross feeds	$+2.8$ -2.6	$+0.7$ -0.7
PID PDF	$+3.0$ -1.8	$+4.0$ -1.4
ε Correction	$+1.4$ -1.4	$+2.0$ -2.0

conservative, and has negligible effect on the final result, which is largely statistically limited.

In conclusion, we have measured the ratio of the decay rates for $B^- \to D^{*0}K^-$ and $B^- \to D^{*0}\pi^-$ processes with non-CP eigenstates. This constitutes the most precise measurement for this channel. We have also performed the first measurement of the same ratio and of the CP asymmetry A_{CP+}^* for D^0 mesons decaying to CP eigenstates. These results, together with measurements exploiting $B^- \to D^0K^-$, $B^- \to D^0K^{*-}$ and $B^- \to D^{*0}K^{*-}$ decays [2,10], constitute a first step towards measuring the angle γ. Furthermore, assuming factorization and flavor-SU(3) symmetry, theoretical calculations (in the tree-level approximation) predict: $\mathcal{B}(B^- \to D^{*0}K^-)/\mathcal{B}(B^- \to D^{*0}\pi^-) \sim (V_{us}/V_{ud})^2(f_K/f_\pi)^2 \sim 0.074$, where f_K and f_π are the meson decay constants [11]. Our results accord with these predictions.

[1] M. Gronau and D. Wyler, Phys. Lett. B **265**, 172 (1991); M. Gronau and D. London, Phys. Lett. B **253**, 483 (1991); D. Atwood, I. Dunietz, and A. Soni, Phys. Rev. Lett. **78**, 3257 (1997); A. Soffer, Phys. Rev. D **60**, 054032 (1999); M. Gronau, Phys. Rev. D **58**, 037301 (1998); Z. Xing, Phys. Rev. D **58**, 093005 (1998); J. H. Jang and P. Ko, Phys. Rev. D **58**, 111302 (1998); M. Gronau and J. L. Rosner, Phys. Lett. B **439**, 171 (1998).

[2] Belle Collaboration, K. Abe *et al.*, Phys. Rev. Lett. **87**, 111801 (2001).

[3] *BABAR* Collaboration, B. Aubert *et al.*, Nucl. Instrum. Methods Phys. Res., Sect. A **479**, 1 (2002).

[4] GEANT4 Collaboration, S. Agostinelli *et al.*, Nucl. Instrum. Methods Phys. Res., Sect. A **506**, 250 (2003).

[5] E691 Collaboration, J. C. Anjos *et al.*, Phys. Rev. D **48**, 56 (1993).

[6] A. Bondar and T. Gershon, Phys. Rev. D **70**, 091503 (2004).

[7] K. S. Cranmer, Comput. Phys. Commun. **136**, 198 (2001).

[8] ARGUS Collaboration, H. Albrecht *et al.*, Z. Phys. C **48**, 543 (1990).

[9] F. James, Comput. Phys. Commun. **10**, 343 (1975).

[10] *BABAR* Collaboration, B. Aubert *et al.*, Phys. Rev. D **69**, 051101 (2004); *BABAR* Collaboration, B. Aubert *et al.*, Phys. Rev. Lett. **92**, 202002 (2004); *BABAR* Collaboration, B. Aubert *et al.*, Phys. Rev. Lett. **92**, 141801 (2004); Belle Collaboration, S. K. Swain *et al.*, Phys. Rev. D **68**, 051101 (2003).

[11] M. Gronau *et al.*, Phys. Rev. D **52**, 6356 (1995).